OncoTargets and Therapy

Dovepress
open access to scientific and medical research

Open Access Full Text Article

ORIGINAL RESEARCH

^{18}F-FHBG PET-CT Reporter Gene Imaging of Adoptive CIK Cell Transfer Immunotherapy for Breast Cancer in a Mouse Model

This article was published in the following Dove Press journal:
OncoTargets and Therapy

Xiaofeng Li[1–3,*]
Guotao Yin[1–3,*]
Wei Ji[2–4,*]
Jianjing Liu[1–3]
Yufan Zhang[1–3]
Jian Wang[1–3]
Xiang Zhu[1–3]
Lei Zhu[1–3]
Dong Dai[1–3]
Wenchao Ma[1–3]
Wengui Xu[1–3]

[1]Department of Molecular Imaging and Nuclear Medicine, Tianjin Medical University Cancer Institute and Hospital, National Clinical Research Center for Cancer, Tianjin 300060, People's Republic of China; [2]Key Laboratory of Cancer Prevention and Therapy, Tianjin Medical University Cancer Institute and Hospital, Tianjin, 300060, People's Republic of China; [3]Tianjin's Clinical Research Center for Cancer, Tianjin Medical University Cancer Institute and Hospital, Tianjin, 300060, People's Republic of China; [4]Public Laboratory, Tianjin Medical University Cancer Institute and Hospital, National Clinical Research Center for Cancer, Tianjin 300060, People's Republic of China

*These authors contributed equally to this work

Correspondence: Wengui Xu
Department of Molecular Imaging and Nuclear Medicine, Tianjin Medical University Cancer Institute and Hospital, National Clinical Research Center for Cancer, Huan-Hu-Xi Road, Ti-Yuan-Bei, He Xi District, Tianjin 300060, People's Republic of China
Tel +86 22 23340123
Fax +86-22-23359337
Email wenguixy@yeah.net

Background: To further improve the efficiency of adoptively transferred cytokine-induced killer (CIK) cell immunotherapy in breast cancer (BC), a reliable imaging method is required to visualize and monitor these transferred cells in vivo.

Methods: Herpes simplex virus 1-thymidine kinase (*HSV1-TK*) and 9-(4-[^{18}F]fluoro-3-(hydroxymethyl)butyl)guanine (^{18}F-FHBG) were used as a pair of reporter gene/reporter probe for positron emission tomography (PET) imaging in this study. Following the establishment of subcutaneous BC xenograft-bearing nude mice models, induced human CIK cells expressing reporter gene *HSV1-TK* through lentiviral transduction were intravenously injected to nude mice. γ-radioimmunoassay was used to determine the specific uptake of ^{18}F-FHBG by these genetically engineered CIK cells expressing *HSV1-TK* in vitro, and ^{18}F-FHBG micro positron emission tomography-computed tomography (PET-CT) imaging was performed to visualize these adoptively transferred CIK cells in tumor-bearing nude mice.

Results: Specific uptake of ^{18}F-FHBG by CIK cells expressing *HSV1-TK* was clearly observed in vitro. Consistently, the localization of adoptively transferred CIK cells in tumor target could be effectively visualized by ^{18}F-FHBG micro PET-CT reporter gene imaging.

Conclusion: PET-CT reporter gene imaging using ^{18}F-FHBG as a reporter probe enables the visualization and monitoring of adoptively transferred CIK cells in vivo.

Keywords: breast cancer, CIK immunotherapy, HSV1-TK, reporter gene, ^{18}F-FHBG PET-CT

Introduction

As reported in cancer statistics, breast cancer (BC) is one of the most common female malignancies worldwide and the leading cause of cancer-related mortality among women globally, ranking first in prevalence and second in mortality.[1] With the development of early diagnostic techniques and the emergence of more effective molecular targeted therapeutic drugs, such as tamoxifen[2] and trastuzumab,[3] the efficiency of breast cancer treatment has improved and the survival rate for breast cancer patients has increased markedly during the past decades.[4,5] However, to further improve the efficiency of breast cancer treatment is a new challenge due to the development of treatment resistance and side effects.[6–8]

Currently, immunotherapy is considered as a promising treatment option for cancer,[9] and adoptive cytokine-induced killer (CIK) cell transfer is commonly used

in a variety of tumor immunotherapeutic strategies due to its advantage.[10–14] CIK cells are induced by culturing peripheral blood mononuclear cells (PBMCs) with the addition of an anti-*CD3* antibody, recombinant human interleukin (rh*IL-1α*), recombinant human interferon gamma (rh*IFN-γ*) and recombinant human interleukin-2 (rh*IL-2*), and mainly consist of a $CD3^+$ T cell population which simultaneously express a natural killer cell marker *CD56*.[14] In contrast with other adoptive cell transfer immunotherapies using other subsets of immunologic effector cells, such as tumor-infiltrating lymphocytes, cytotoxic T cells and γδ T cells,[15–17] CIK cells tend to proliferate rapidly in vitro and exhibit a strong non-major histocompatibility complex-restricted cytolytic activity. Furthermore, a growing number of studies have indicated that CIK cells could also play an important role in recurrence prevention by killing cancer stem cells and regulating the anti-tumor immune surveillance.[18,19]

Nevertheless, acquired resistance to immunotherapy may limit responses to such treatment.[20,21] A longitudinal assessment of those adoptively transferred immune effector cells,[22,23] including cells localization, homing, tumor targeting, retention, and immune cell engagement with the tumor cells, would be beneficial to optimize immunotherapy by screening potentially sensitive patients, predicting and evaluating the responses to treatment based on some valuable early indicators. As a molecular functional imaging modality, the dual scans of molecularly functional PET imaging and anatomical CT imaging allow for a precise measurement of intracellular activities by tracking the accumulation of positron-emitting radio-labeled probes in targeted tissues.[24,25] Even though direct ex vivo cell labeling for visualizing adoptively transferred cells in vivo is a relatively easy and well-established methodology,[26] an extensive application of this imaging paradigm in clinical practice is limited by a small window of opportunity to monitor immune cells trafficking in vivo, which is due to radioactivity dilution caused by radiolabel decay, cell division and biological clearance (Ponomarev et al 2009).[27] In that case, long half-life radionuclides such as ^{131}I, ^{89}Zr, and ^{64}Cu can really help to enable a longer period of monitoring.[28–30] However, high levels of radiotracer concentration can impair the biological function of radiolabeled adoptively transferred immune cells.[22,23,27] Whereas indirect labeling of adoptively transferred cells using a PET reporter gene/reporter probe imaging paradigm is able to effectively monitor cellular immunotherapy in vivo in the absence of high levels of radiotracer concentration.[31] The PET reporter gene imaging paradigm involves an ex vivo genetically engineering of the adoptively transferred cells to integrate the reporter gene into cell DNAs in advance before adoptive cellular therapy.[27] Herpes simplex virus type-1 thymidine kinase gene (*HSV1-TK*) and 9-(4-[^{18}F]fluoro-3-(hydroxymethyl)butyl)guanine (^{18}F-FHBG) is one of the most commonly used paired reporter gene/reporter probe in PET reporter gene imaging of tumor immunotherapy.[32,33]

In the present investigation, induced CIK cells with reporter gene *HSV1-TK* expression were intravenously injected into established subcutaneous xenograft-bearing nude mouse models nude mice models, and then ^{18}F-FHBG micro PET-CT imaging was performed to preliminarily evaluate the tumor targeting of these adoptively transferred CIK cells in vivo.

Materials and Methods

Cell Culture

The human breast cancer cell line T47D and human embryonic kidney cell line HEK293T were kindly provided by the Central Laboratory, Tianjin Medical University Cancer Institute and Hospital. Cell culture reagents, including culture media Dulbecco's Modified Eagle Medium (DMEM), fetal bovine serum (FBS), antibiotics (streptomycin and penicillin) were all purchased from GIBCO (Thermo Fisher Scientific, Inc., Carlsbad, CA). T47D cells were regularly cultured in DMEM supplemented with 10% FBS and 1% streptomycin and penicillin in a 5% CO_2 humidified incubator at 37°C.

CIK Cell Preparation and Flow Cytometry

Human peripheral blood samples were obtained from healthy volunteer blood donors of blood (Tianjin Blood Center). PBMCs were isolated by centrifugation on Ficoll density gradients (GE Healthcare Life Sciences, Shanghai, China). To induce CIK cells, PBMCs were incubated in serum-free medium GT-T551 (Takara, Japan) containing 100 ng/mL anti-*CD3* antibody (e-Bioscience, San Diego, USA), 100 U/mL rhIL-1α, and 1000 U/mL rh*IFN-γ* (R&D system, Inc, Minneapolis, MN) on day 1. Subsequently, 200 U/mL rh*IL-2* was added to the medium on day 2, and the medium was regularly replaced with fresh *IFN-γ*- and *IL-2*-containing medium every 3–5 days. On day 14, cells were harvested and analyzed for the phenotypes of CIK cells by flow cytometric assay. Briefly, the phenotypes of induced CIK cells were detected through flow cytometry

using a series of fluorescence-labeled monoclonal antibodies specific for *CD3, CD4, CD8, CD25, CD127, CD16/CD56, CD45RA, CD45RO* (eBioscience, San Diego, CA). Induced CIK cells (5×10^5) were incubated with these antibodies for 30 min on ice, and then cells were washed twice and analyzed on Fluorescence-Activated Cell Sorting (FACS) Aria I (BD Biosciences, San Diego, CA, USA) by using CellQuest software (BD Biosciences, San Diego, CA, USA).

Lentivirus Packaging and Lentiviral Transduction of T47D and CIK Cells

Prior to lentivirus packaging and lentiviral transduction, a full-length cDNA for herpes simplex virus 1-thymidine kinase (*HSV1-TK*) was cloned into a pLVX5-*GFP* lentiviral vector (Suzhou Genepharma Co., Ltd, Nanjing, China). Lentiviral particles were produced by transient co-transfection of HEK293T cells with pSPAX2, pMD2.G vectors plus pLVX5-*GFP-HSV1-TK* vector or the empty vector pLVX5-*GFP*. The lentiviral particles supernatant was collected 48 hours afterwards and the viral titer was determined through infection of 293T cells with limiting dilutions of supernatant. For lentiviral transduction of T47D cells and induced CIK cells, one single round of transduction with lentiviral particles was performed at a MOI (multiplicity of infection) of 10 (for T47D) or 100 (for CIK cells) in the presence of 5μg/mL PolyBrene (sigma-Aldrich, Oakville, Canada). Following lentiviral transduction, cells were continually cultured in complete medium for 5–8 days, and the proportion of *GFP*-positive cell population in CIK cell culture was then used to evaluate the efficiency of lentiviral transduction.

Radiosynthesis of 9-(4-[^{18}F]Fluoro-3-(Hydroxymethyl)Butyl)Guanine (^{18}F-FHBG)

The one-pot, two-step radiosynthesis of ^{18}F-FHBG was performed in the department of molecular imaging and nuclear medicine in our institute. Monomethoxytri-tyl-9-[4-(tosyl)-3-monomethoxytrityl-methylbutyl] guanine, the precursor of ^{18}F-FHBG was purchased from J & K Scientific LTD (Beijing, China). Nucleophilic substitution method was applied to accomplish a fully automatic labeling of ^{18}F-FHBG by TraceLAB Fx-FN synthesizer (General Electric Healthcare, Waukesha, WI, United States). Briefly, [^{18}F] Fluoride was produced in our department by the ^{18}O(p, n) ^{18}F reaction through proton irradiation of enriched (95%) ^{18}O water using MiniTrace cyclotron (General Electric Healthcare, Waukesha, WI, United States). K_2CO_3 (0.5 mL, 0.04 M) and Kryptofix 2.2.2 (1 mL, 20 mg/mL) were added to attain F-18 residue. After the final drying sequence, 2–3 mg of N2, monomethoxytrityl-9-[4-(tosyl)-3-monomethoxytrityl-methylbutyl] guanine (1) dissolved in 0.9 mL DMSO were added to the F-18 residue. The contents were briefly mixed (vortex) before being subjected to microwave irradiation. After the last heating and cooling, 1mL 1N HCl was added and the mixture was heated for 10 min at 110°C. After the reaction mixture had cooled, it was neutralized with 0.6 mL 1 N NaOH. All solutions in the reaction were further purified via C18 HPLC with flow phase NH_4OAc (50 mmol/L): C_2H_5OH = 93:7, flow rate 5 mL/min and ultraviolet 254 nm. Product retention time is about 30 min. Finally, the obtained product was sterilized via passing through a 0.22 μm microporous membrane, and the radioactivity was also measured by an activity meter. Generally, the radioactivity of ^{18}F-FHBG synthesized in our institution was about 1.11×10^8 Bq/mL.

Detection of ^{18}F-FHBG Uptake by Lentivirally Transduced Cells Expressing HSV1-TK in vitro

To determine the specific uptake of ^{18}F-FHBG by T47D cells and CIK cells which were lentivirally transduced to express HSV1-TK, the culture media (12-well culture plate) were replaced with fresh medium containing 1.11×10^7 Bq ^{18}F-FHBG for different durations (0.5, 1, and 2 h). Rinsing, digestion and washing with PBS were performed after incubation to eliminate extracellular radioactivity in the medium. Then, single-cell suspensions were prepared in PBS to detect ^{18}F-FHBG uptake by T47D cells and CIK cells through the radioactivity counting with a γ-radioimmunoassay counter (Cobra Quantum; Packard). The results were expressed as the radioactivity counts per minute (CPM) per 1×10^5 cells.

^{18}F-FHBG Micro PET-CT Imaging

BALB/c nude mice (aged ~6 weeks, Jiangsu GemPharmatech Co. Ltd, Nanjing, China) with an average body weight of 20 g were purchased and housed under pathogen-free conditions in this present investigation. Human breast cancer xenografts were established by subcutaneous injection of lentivirally transduced T47D cells (200 μL, 1×10^7/mL) in bilateral axilla of nude mice with left xenografts for a negative expression of *HSV1-TK* and

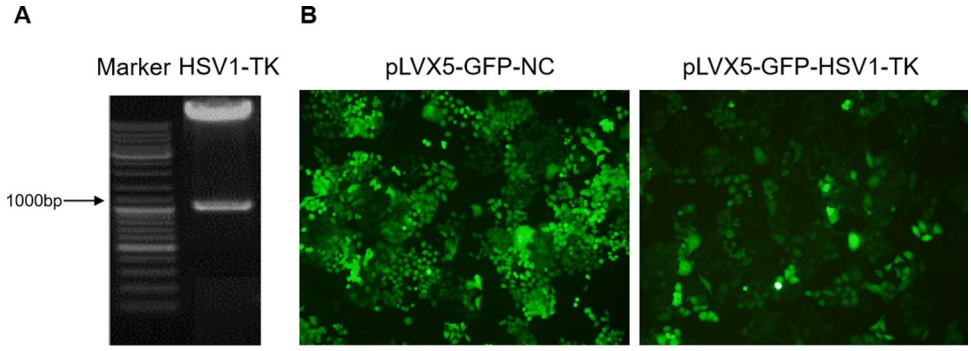

Figure 1 Lentiviral transduction of breast cancer cell T47D to express reporter gene *HSV1-TK*. (**A**) A restriction endonuclease digestion analysis was performed to identify the successful cloning of *HSV1-TK* into lentiviral vector pLVX5-*GFP*. A specific band at the location corresponding to 1131 bp was clearly visible. (**B**) *GFP* was used to indirectly determine the efficiency of lentiviral transduction of breast cancer cell T47D. Under a fluorescent microscope, up to 90–95% of T47D cells were positive for *GFP* expression, demonstrating the success of control (pLVX5-*GFP*-NC) and HSV1-TK (pLVX5-*GFP-HSV1-TK*) lentiviral transduction.
Abbreviations: HSV1-TK, herpes simplex virus 1-thymidine kinase; GFP, green fluorescent protein.

right xenografts for positive expression of *HSV1-TK*, respectively. One hour after intravenous injections of ^{18}F-FHBG at a concentration of 3.7 × 10^5 Bq/g, micro PET-CT imaging (Inveon PET.SPETCT.CT, SIEMENS, Germany) was performed for three representative nude mice to test the ^{18}F-FHBG (reporter probe)/*HSV1-TK* (reporter gene) system in vivo. For ^{18}F-FHBG PET-CT imaging of CIK cells, a total of 8 breast cancer T47D xenografts without HSV1-TK expression were initiated by subcutaneously injecting nude mice in right axilla with T47D cells (200 μL, 1 × 10^7/mL). When the xenografts grew to a maximal diameter of 10–15mm, lentivirally transduced CIK cells (200 μL, 2 × 10^7/mL) with *HSV1-TK* expression or not were intravenously injected to xenograft-bearing nude mice, with 4 mice in each group. Approximately 24 h after the intravenous injection of CIK cells, ^{18}F-FHBG micro PET-CT imaging was performed following intravenous injections of ^{18}F-FHBG. Briefly, CT (Voltage = 80 kV, Current = 500 μA) was performed followed by PET scanning (Inveon PET. SPETCT.CT, SIEMENS, Germany), and the total scanning time for both procedures was about 30 min. The separate PET images and CT images acquired were transferred to a workstation for image reconstruction and image fusion using iteration method (COBRA_ Exxim: Licensed to Siemens; Ineon Research Workplace), and the maximal standard uptake values (SUVmax) of the xenografts were calculated as main outcome measurements.

Statistical Analyses

Data are presented as the mean ± standard deviation (SD) in this study. The significance of the differences between group means was determined using paired or unpaired Student's *t*-test with GraphPad Prism software version 5.0 (GraphPad, La Jolla, CA). A P-value under 0.05 was considered to indicate a statistically significant difference.

Results

pLVX5-GFP-HSV1-TK Lentivirus Packaging and Lentiviral Transduction of Breast Cancer Cell T47D

Restriction endonuclease digestion analysis (NotI and BamHI) of the lentiviral vector (pLVX5-*GFP-HSV1-TK*) was performed to identify *HSV1-TK* band at the location corresponding to 1131 bp (Figure 1A). Following lentivirus packaging and lentiviral particle collection, lentiviral transduction was performed to obtain T47D cells expressing reporter gene *HSV1-TK*. As shown in Figure 1B, up to 90–95% GFP-positive T47D cells were identified in a fluorescence microscope field, which demonstrated the success of lentiviral vector transfection and lentiviral transduction.

CIK Cells Preparation and Lentiviral Transduction of CIK Cells

Induced CIK cells were harvested and analyzed for the phenotype of CIK cells by flow cytometric assay (Figure 2A). Usually, CIK cells expand almost 100 times after being induced and having proliferated in vitro for 2 weeks. As illustrated in Figure 2A and Table 1, the majority of the induced CIK cells were composed of $CD3^+CD8^+$ and $CD3^+CD16^+CD56^+$ cell populations, which is consistent with previous reports. Meanwhile, a higher proportion of $CD45RO^+$ cell population and a lower proportion of $CD45RA^+$ cell population in cultured CIK cells suggest a highly activated phenotype. However, regulatory

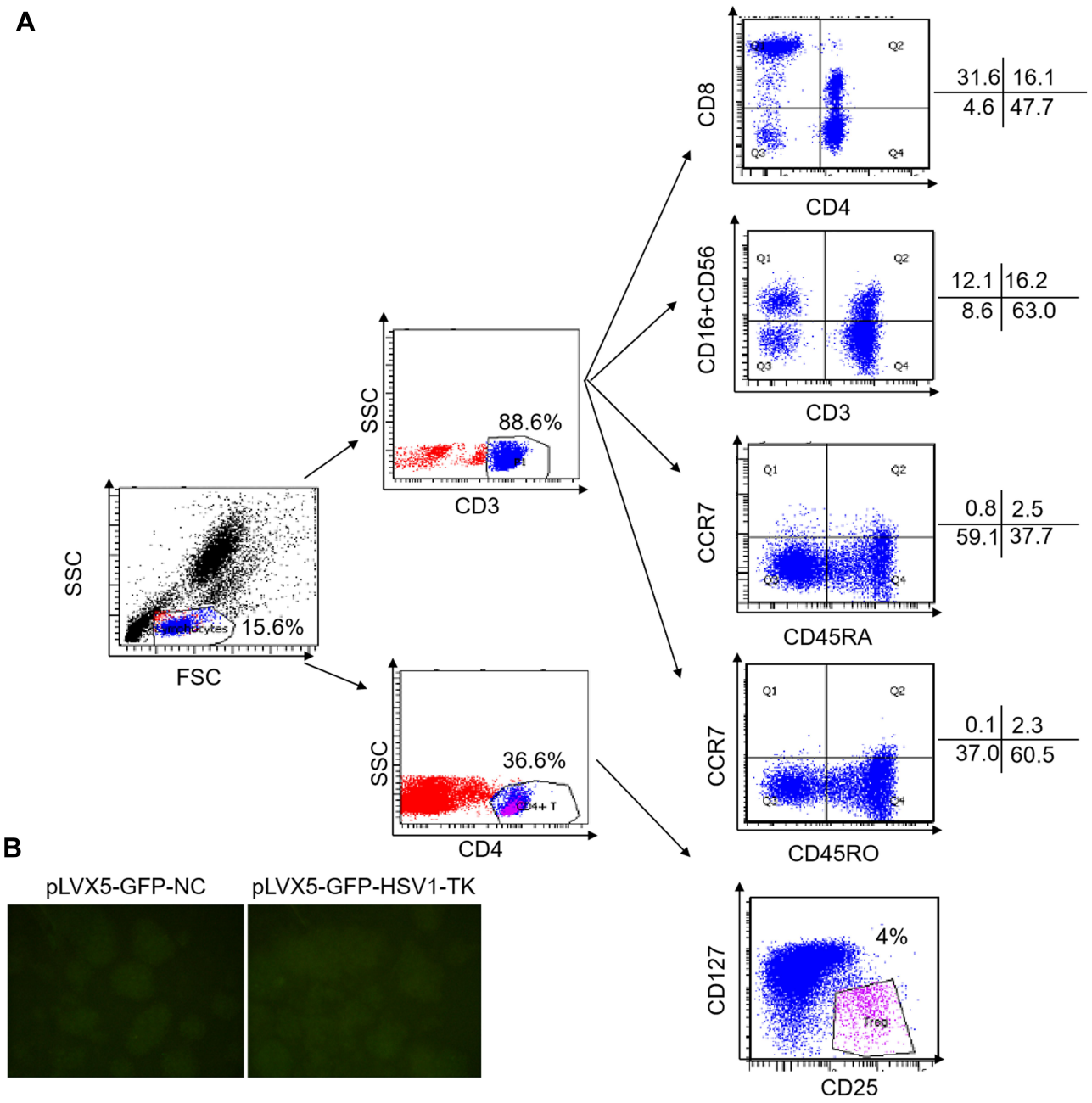

Figure 2 The phenotype of the induced CIK cells was detected by flow cytometric assay. (**A**) Several representative flow cytometry scatter plots demonstrated that the induced CIK cells were mostly with activated phenotype (*CD45RO*) and mainly composed of $CD3^+CD8^+$ and $CD3^+$T cells with natural killer (NK) cell marker (*CD16*/*CD56*), whereas Tregs were not significantly increased during this period of CIK cells induction and expansion. (**B**) GFP was used to indirectly determine the efficiency of lentiviral transduction in CIK cells. Under a fluorescent microscope, up to 90–95% of CIK cells were positive for GFP expression, demonstrating the success of control (pLVX5-*GFP*-NC) and HSV1-TK (pLVX5-*GFP-HSV1-TK*) lentiviral transduction.
Abbreviations: CIK, cytokine-induced killer; NK, natural killer; GFP, green fluorescent protein; NC, negative control.

T (Treg) cell phenotypes ($CD25^+CD127^-$) were not significantly increased during this period of CIK cells induction and expansion, with 1–5% of primary PBMCs reported to be Treg cells. As shown in Figure 2B, one single round of lentiviral transduction of CIK cells resulted in 90–95% GFP-positive CIK cells in a fluorescence microscope field, suggesting a successful lentiviral transduction of CIK cells. CIK cells preparation, lentiviral transduction and associated flow cytometric analyses were all repeated for three times using isolated PBMCs from three different healthy donors.

Table 1 Flow Cytometric Analysis of the Phenotype of Induced CIK Cells

Phenotype	Proportion of Induced CIK Cells (%)
$CD3^+$	86.34±10.63
$CD4^+$	41.65±6.34
$CD8^+$	56.38±8.37
$CD16^+/CD56^+$	38.74±3.45
$CD45RA^+$	29.64±3.64
$CD45RO^+$	68.71±2.75
$CD25^+/CD127^-$	3.97±1.09

^{18}F-FHBG Uptake by Lentivirally Transduced T47D Cells and CIK Cells Expressing HSV1-TK

Lentiviral transduced T47D cells and CIK cells were incubated with ^{18}F-FHBG in culture media for different durations (0.5, 1, and 2 h) to investigate the specific uptake of ^{18}F-FHBG by cells expressing *HSV1-TK* in vitro by γ-radioimmunoassay. As demonstrated in Figure 3, ^{18}F-FHBG uptakes by T47D cells and CIK cells expressing *HSV1-TK* were markedly higher than that by control cells without *HSV1-TK* expression ($P < 0.0001$), suggesting a specific uptake of ^{18}F-FHBG by cells expressing *HSV1-TK* in vitro. The maximal radioactivity counting was observed in cell samples with incubation for 1 h.

^{18}F-FHBG Micro PET-CT Imaging of the Tumor Targeting of Adoptively Transferred CIK Cells in Nude Mice Models Bearing T47D Xenografts

^{18}F-FHBG micro PET-CT imaging was performed following intravenous injections of ^{18}F-FHBG to preliminarily evaluate the tumor targeting of adoptively transferred CIK cells in T47D xenograft-bearing nude mouse models. SUVmax was used to semiquantitatively analyze the radioactivity in target region of interest. As expected, ^{18}F-FHBG specifically accumulated in xenografts derived from T47D cells which were lentivirally transduced to express *HSV1-TK* (Figure 4A), whereas the ^{18}F-FHBG uptake by control T47D xenograft was significantly lower ($P = 0.0071$) than that in the T47D xenograft expressing *HSV1-TK*. In contrast to the weak ^{18}F-FHBG accumulation in T47D xenograft that had received an intravenous injection of control lentivirally transduced CIK cells without *HSV1-TK* expression (Figure 4B), obvious ^{18}F-FHBG accumulations were observed in a T47D xenograft that had received an intravenous injection of lentivirally transduced CIK cells expressing *HSV1-TK* ($P = 0.0155$). These results highly suggested that the localization of adoptively transferred CIK cells in tumor target could be effectively visualized by micro PET-CT imaging using *HSV1-TK* and ^{18}F-FHBG as a reporter gene and reporter tracer, respectively.

Discussion

Despite the significant progress that has been made in the development of anti-tumor drugs for breast cancer over the past few decades, especially in targeted therapy,[2,3,5] the majority of cancer patients may relapse and suffer from serious side effects caused by these innovative treatments.[6–8] In recent years, immunotherapy, particularly for adoptive CIK cell transfer, has become an important neoadjuvant therapeutic approach for breast cancer treatment.[9–11,14] To further improve the significant promise of adoptively transferred CIK cells immunotherapy, a noninvasive and tomographic method is required to visualize and monitor these transferred cells in -vivo.[22,23] PET imaging with a pair of nuclear reporter gene and

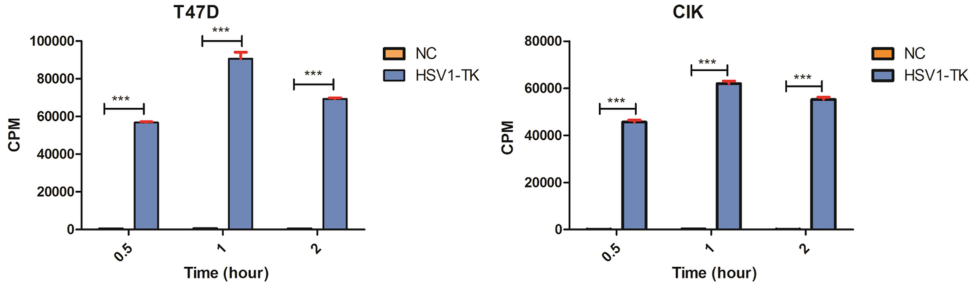

Figure 3 Specific ^{18}F-FHBG uptake by lentivirally transduced T47D cells and CIK cells expressing *HSV1-TK*. Following incubation with ^{18}F-FHBG in culture media for different durations (0.5, 1, and 2 h), a γ-radioimmunoassay was performed to investigate the specific ^{18}F-FHBG uptake by lentivirally transduced T47D (left) and CIK cells (right) expressing *HSV1-TK*. Three independent experiments were performed for quantitative analyses. As shown, *HSV1-TK* overexpression via lentiviral transduction enabled a specific ^{18}F-FHBG uptake by cells expressing *HSV1-TK* in vitro ($P < 0.0001$). The maximal radioactivity counting were observed for samples with incubation for 1 h. ***$P < 0.001$.

Abbreviations: ^{18}F-FHBG, 9-(4-[^{18}F]fluoro-3-(hydroxymethyl)butyl)guanine; CIK, cytokine-induced killer; HSV1-TK, herpes simplex virus 1-thymidine kinase.

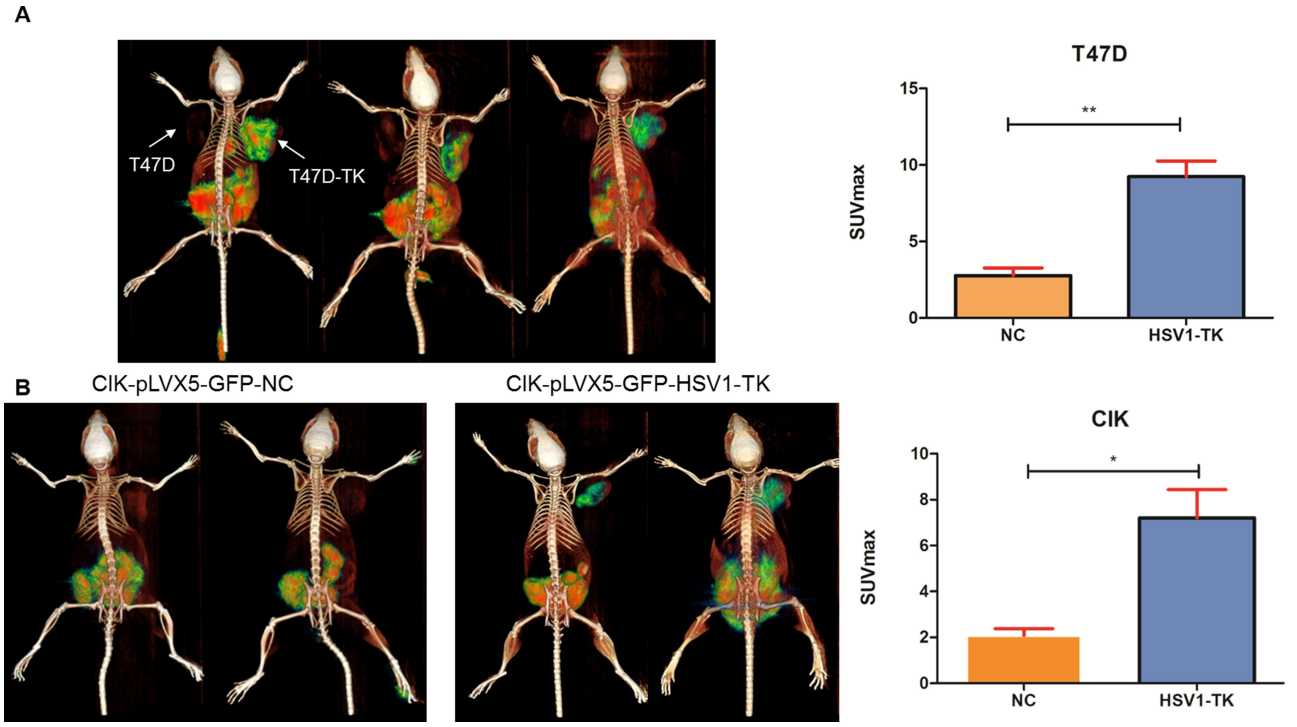

Figure 4 ^{18}F-FHBG micro PET/CT reporter gene imaging of adoptively transferred CIK cells in T47D xenografts-bearing nude mouse models. (**A**) ^{18}F-FHBG micro-PET/CT imaging of xenografts derived from T47D were first performed to confirm the specific uptake of ^{18}F-FHBG by T47D cells expressing *HSV1-TK* in vivo. In contrast with low ^{18}F-FHBG uptake in control T47D xenografts, ^{18}F-FHBG specifically accumulated in T47D-TK xenografts expressing *HSV1-TK*. Three representative ^{18}F-FHBG micro PET/CT images are shown. As shown in the histogram, the SUVmax of T47D xenografts expressing *HSV1-TK* were significantly higher (P = 0.0071) than that of control T47D xenografts (NC). (**B**) The tumor targeting of adoptively transferred CIK cells T47D xenografts-bearing nude mouse models could be effectively visualized by ^{18}F-FHBG micro-PET/CT imaging if the intravenous injection of CIK cells were lentivirally transduced to express reporter gene *HSV1-TK*. Two representative ^{18}F-FHBG micro PET/CT image are shown for each group. As shown in the histogram, the SUVmax of T47D xenografts that had received an intravenous injection of *HSV1-TK*-expressing CIK cells (*HSV1-TK*) were significantly higher (P = 0.0155) than that of T47D xenografts with intravenous injection of control CIK cells (NC). *P < 0.05, **P < 0.01.
Abbreviations: ^{18}F-FHBG, 9-(4-[^{18}F]fluoro-3-(hydroxymethyl)butyl)guanine; PET/CT, positron emission tomography/computed tomography; SUVmax, maximal standard uptake values; HSV1-TK, herpes simplex virus 1-thymidine kinase; CIK, cytokine-induced killer; NC, negative control.

reporter probe is such a modality that allows for a stable, reliable, harmless visualization and monitoring of these cells in vivo.[27,31–33] In the present study, CIK cells which were lentivirally transduced to express reporter gene *HSV1-TK* were transferred into breast cancer T47D-bearing nude mice. One day after an intravenous injection of CIK cells, ^{18}F-FHBG micro PET-CT imaging was performed to visualize the specific localization of these transferred CIK cells in xenografts in vivo. It was found that the localization of adoptively transferred CIK cells in tumor targets could be effectively visualized by ^{18}F-FHBG micro PET-CT reporter gene imaging. Based on the visualization of tumor cellular therapy, some combination treatment involving tumor immunotherapy and tumor gene therapy is able to bring prospect for clinical tumor management. Furthermore, this encouraging finding confirmed the ability of CIK cells to selectively target tumor site, which was potentially applied in suicide gene therapy by using CIK cells as an effective tumor targeting cell vehicle to carry the suicide gene HSV1-TK to the tumor site. Subsequently, based on the direct cytotoxicity and bystander effect induced by suicide gene HSV1-TK, a promising anti-tumor effect is expected in the presence of acyclovir (ACV) or ganciclovir (GCV).

Each imaging technique has its inherent advantage. One advantage of PET imaging over alternative imaging modalities is the flexibility in specific probe design and probe radiolabeling to assess a variety of biological processes.[25] Currently, PET reporter genes generally fall into three distinct categories:[23,34] transporter, receptor and enzymatic. Among them, enzymatic reporters have been the most commonly investigated, especially for herpes simplex virus thymidine kinase (*HSV-TK*) and variants[35] which has been translated into clinical use (NCI clinical trial, NCT01082926).[36] The corresponding PET reporter probes for *HSV1-TK*, such as ^{18}F-FHBG, ^{18}F-FEAU and ^{18}F-FIAU, were reported to be able to track the location and infiltration of tumor-reactive T cell receptor (TCR) or chimeric antigen receptor (CAR)-engineered T cells in preclinical model.[31] However, the major limitation for PET reporter gene imaging is the risk of immunogenicity

and a potential impairment in the function of the reporter cells caused by the ectopic expression of a foreign protein. As previously reported, the induced expression of *HSV1-TK* was immunogenic in patients with $CD8^+$ T cells against the *HSV1-TK* gene.[37] In contrast, no immunogenicity to *HSV1-TK* was observed in preclinical mouse model, which make it useful as a preclinical tool in PET imaging of tumor cellular immunotherapy.[23,27,31,33] With regard to the issue about immunogenicity, a variety of humanized reporter genes have been found to minimize the induced host immune response against reporter genes,[38] such as human norepinephrine transporter (h*NET*),[39] the type 2 human somatostatin receptor (h*SSTr*2)[40] and human deoxycytidine kinase (h*dCK*).[41] In fact, *HSV1-TK* demonstrated a dual function: as a PET reporter gene at low doses and as an effective suicide gene at pharmacologic doses which allows for selective reporter cells elimination in case of adverse effects.[35] The future direction of PET reporter gene imaging of tumor immunotherapy is to apply the induced reporter system in targeted imaging of specific subsets of adoptively transferred immune cells by using lineage-specific promotor.[42,43] The similar induced reporter system may be beneficial to assess the outcome of adoptive cellular immunotherapy.

Apart from PET imaging of tumor immunotherapy with a reporter gene/reporter probe paradigm, in vivo immune cell labeling using radiolabeled proteins is also a promising modality to visualize and monitor anti-tumor immune response or tumor immunotherapy.[23] The designed protein-based radiotracer includes specific antibodies to all antigens of interest or alternate protein scaffolds with protein engineering and molecular evolution strategies, such as nanobody,[42] affibody[44] and cyclic peptides.[45] Cell-specific lineage markers and activation markers are potential-targeted biomarker for PET detection of tumor immunotherapy.[43,46] Antibody-based probes for immuno-PET imaging of anti-*CTLA-4*[47] and *PD-L1*[48] have already been reported and developments of other protein-based targeted molecular imaging agents are expected in the future, which may facilitate predicting or assessing anti-tumor immune response in vivo.

Several limitations should be addressed in this study. First, a dynamic micro PET-CT imaging at various time points after an intravenous injection of lentivirally transduced CIK cells should be performed to dynamically visualize and monitor the trafficking, persistence and engagement with tumor cells of these transferred effector cells. Secondly, to facilitate the establishment of human breast cancer xenografts and the injection of induced human CIK cells to tumor-bearing mouse models, immunodeficient nude mice were used in this study. Therefore, a direct assessment of anti-tumor immune responses in vivo is limited. Lastly, the suicide potential and bystander effect of the PET reporter gene *HSV1-TK* were not tested herein. To summarize, this is a preliminary study about PET imaging of tumor immunotherapy in an experimental setting. The development of human-derived reporter genes with low or no immunogenicity and direct immuno-PET imaging of the unique endogenous biochemical signature of activated immune cells will be markedly helpful in the clinical application of PET detection of anti-tumor immune response and tumor immunotherapy.

Conclusion

Immunotherapy, particularly for adoptive CIK cells transfer, has become an important neoadjuvant therapeutic option for breast cancer treatment. A stable and reliable visualization and monitoring of these transferred cells in vivo by means of a noninvasive and tomographic method would be beneficial to optimize the efficiency of this therapy. In the present investigation, PET-CT reporter gene imaging using ^{18}F-FHBG as a reporter probe demonstrated that these transferred CIK cells could be specifically localized and visualized in xenografts in vivo.

Compliance with Ethical Standards

All protocols involving animals were in strict accordance with guidelines for the Care and Use of Experimental Animals of the National Institutes of Health. The use of cell line T47D and HEK293T and all animal experiments were approved by the Ethical Review Committee of Tianjin Medical University Cancer Institute and Hospital. In addition, the collection of blood samples was approved by Ethics Review Committee of Tianjin Blood Center and agreed by healthy volunteer donors with written informed consent in accordance with the declaration of Helsinki and relevant approved guidelines.

Acknowledgments

This work was supported by grants from the National Natural Science Foundation of China (grant nos. 81601377, 2018ZX09201015, 2017ZX09304021), the Tianjin Science and Technology committee Fund (grant nos. 18PTZWHZ00100 and H2018206600), the Science & Technology Development Fund of Tianjin Education

Commission for Higher Education (grant nos. 2018KJ057 and 2018KJ061).

Disclosure

The authors declare that they have no conflicts of interest to declare for this study. The abstract of this paper was presented at the SNMMI 2020 Annual Meeting as a poster presentation with interim findings. The poster's abstract was published in "Poster Abstracts" in the Journal of Nuclear Medicine: http://jnm.snmjournals.content/61/supplement_1/1065

References

1. Siegel RL, Miller KD, Jemal A. Cancer statistics, 2018. *CA Cancer J Clin*. 2018;68(1):7–30. doi:10.3322/caac.21442
2. Lv F, Jin WH, Zhang XL, Wang ZR, Sun AJ. Tamoxifen therapy benefit predictive signature combining with prognostic signature in surgical-only ER-positive breast cancer. *J Cell Physiol*. 2019;234 (7):11140–11148. doi:10.1002/jcp.27756
3. Schmid S, Klingbiel D, Aebi S, et al. Long-term responders to trastuzumab monotherapy in first-line HER-2+ advanced breast cancer: characteristics and survival data. *BMC Cancer*. 2019;19(1):902. doi:10.1186/s12885-019-6105-3
4. Trapani D, Rajasekar AKA, Mathew A. More options for adjuvant treatment of HER2-positive breast cancer: how to choose wisely? *Int J Cancer*. 2019;145(11):2901–2906. doi:10.1002/ijc.32418
5. Kaczmarek E, Saint-Martin C, Pierga JY, et al. Long-term survival in HER2-positive metastatic breast cancer treated with first-line trastuzumab: results from the french real-life curie database. *Breast Cancer Res*. 2019;178(3):505–512. doi:10.1007/s10549-019-05423-5
6. Barish R, Gates E, Barac A. Trastuzumab-induced cardiomyopathy. *Cardiol Clin*. 2019;37(4):407–418. doi:10.1016/j.ccl.2019.07.005
7. Ge X, Zhao Y, Dong L, Seng J, Zhang X, Dou D. NAMPT regulates PKM2 nuclear location through 14-3-3ζ: conferring resistance to tamoxifen in breast cancer. *J Cell Physiol*. 2019;234 (12):23409–23420. doi:10.1002/jcp.28910
8. Qiu N, He YF, Zhang SM, et al. Cullin7 enhances resistance to trastuzumab therapy in Her2 positive breast cancer via degrading IRS-1 and downregulating IGFBP-3 to activate the PI3K/AKT pathway. *Cancer Lett*. 2019;464:25–36. doi:10.1016/j.canlet.2019.08.008
9. Krasniqi E, Barchiesi G, Pizzuti L, et al. Immunotherapy in HER2-positive breast cancer: state of the art and future perspectives. *J Hematol Oncol*. 2019;12(1):111. doi:10.1186/s13045-019-0798-2
10. Shirjang S, Alizadeh N, Mansoori B, et al. Promising immunotherapy: highlighting cytokine-induced killer cells. *J Cell Biochem*. 2019;120(6):8863–8883. doi:10.1002/jcb.28250
11. Li M, Wang Y, Wei F, et al. Efficiency of cytokine-induced killer cells in combination with chemotherapy for triple-negative breast cancer. *J Breast Cancer*. 2018;21(2):150–157. doi:10.4048/jbc.2018.21.2.150
12. Guo Q, Zhu D, Bu X, et al. Efficient killing of radioresistant breast cancer cells by cytokine-induced killer cells. *Tumour Biol*. 2017;39 (3):1010428317695961. doi:10.1177/1010428317695961
13. Pan K, Guan XX, Li YQ, et al. Clinical activity of adjuvant cytokine-induced killer cell immunotherapy in patients with post-mastectomy triple-negative breast cancer. *Clin Cancer Res*. 2014;20(11):3003–3011. doi:10.1158/1078-0432.ccr-14-0082
14. Hu J, Hu J, Liu X, Hu C, Li M, Han W. Effect and safety of cytokine-induced killer (CIK) cell immunotherapy in patients with breast cancer: a meta-analysis. *Medicine (Baltimore)*. 2017;96(42): e8310. doi:10.1097/md.0000000000008310
15. Sakellariou-Thompson D, Forget MA, Hinchcliff E, et al. Potential clinical application of tumor-infiltrating lymphocyte therapy for ovarian epithelial cancer prior or post-resistance to chemotherapy. *Cancer Immunol Immunother*. 2019;68(11):1747–1757. doi:10.1007/s00262-019-02402-z
16. Peng W, Williams LJ, Xu C, et al. Anti-OX40 antibody directly enhances the function of tumor-reactive CD8+ T cells and synergizes with PI3Kβ inhibition in PTEN loss melanoma. *Clin Cancer Res*. 2019;25(21):6406–6416. doi:10.1158/1078-0432.ccr-19-1259
17. Zou C, Zhao P, Xiao Z, Han X, Fu F, Fu L. γδ T cells in cancer immunotherapy. *Oncotarget*. 2017;8(5):8900–8909. doi:10.18632/oncotarget.13051
18. Yang T, Zhang W, Wang L, et al. Co-culture of dendritic cells and cytokine-induced killer cells effectively suppresses liver cancer stem cell growth by inhibiting pathways in the immune system. *BMC Cancer*. 2018;18(1):984. doi:10.1186/s12885-018-4871-y
19. Song H, Liu S, Zhao Z, et al. Increased cycles of DC/CIK immunotherapy decreases frequency of Tregs in patients with resected NSCLC. *Int Immunopharmacol*. 2017;52:197–202. doi:10.1016/j.intimp.2017.09.014
20. Yazdanifar M, Zhou R, Grover P, et al. Overcoming immunological resistance enhances the efficacy of a novel anti-tMUC1-CAR T cell treatment against pancreatic ductal adenocarcinoma. *Cells*. 2019;8(9): E1070. doi:10.3390/cells8091070
21. Alissafi T, Hatzioannou A, Legaki AI, Varveri A, Verginis P. Balancing cancer immunotherapy and immune-related adverse events: the emerging role of regulatory T cells. *J Autoimmun*. 2019;104:102310. doi:10.1016/j.jaut.2019.102310
22. Tumeh PC, Radu CG, Ribas A. PET imaging of cancer immunotherapy. *J Nucl Med*. 2008;49(6):865–868. doi:10.2967/jnumed.108.051342
23. McCracken MN, Tavaré R, Witte ON, Wu AM. Advances in PET detection of the antitumor T cell response. *Adv Immunol*. 2016;131:187–231. doi:10.1073/pnas.1221840110
24. Paydary K, Seraj SM, Zadeh MZ, et al. The evolving role of FDG-PET/CT in the diagnosis, staging, and treatment of breast cancer. *Mol Imaging Biol*. 2019;21(1):1–10. doi:10.1007/s11307-018-1181-3
25. Phelps ME. Positron emission tomography provides molecular imaging of biological processes. *Proc Natl Acad Sci U S A*. 2000;97 (16):9226–9233. doi:10.1073/pnas.97.16.9226
26. Lacroix S, Egrise D, Van Simaeys G, et al. [^{18}F]-FBEM, a tracer targeting cell-surface protein thiols for cell trafficking imaging. *Contrast Media Mol Imaging*. 2013;8(5):409–416. doi:10.1002/cmmi.1540
27. Ponomarev V. Nuclear imaging of cancer cell therapies. *J Nucl Med*. 2009;50(7):1013–1016. doi:10.1038/sj.neo.7900204
28. Zanzonico P, Koehne G, Gallardo HF, et al. [131I]FIAU labeling of genetically transduced, tumor-reactive lymphocytes: cell-level dosimetry and dose-dependent toxicity. *Eur J Nucl Med Mol Imaging*. 2006;33(9):988–997. doi:10.1007/s00259-005-0057-3
29. Sato N, Wu H, Asiedu KO, Szajek LP, Griffiths GL, Choyke PL. (89) zr-oxine complex PET cell imaging in monitoring cell-based therapies. *Radiology*. 2015;275(2):490–500. doi:10.1148/radiol.15142849
30. Griessinger CM, Maurer A, Kesenheimer C, et al. ^{64}Cu antibody-targeting of the T-cell receptor and subsequent internalization enables in vivo tracking of lymphocytes by PET. *Proc Natl Acad Sci U S A*. 2015;112(4):1161–1166. doi:10.1073/pnas.1418391112
31. Lee JT, Moroz MA, Ponomarev V. Imaging T cell dynamics and function using PET and human nuclear reporter genes. *Methods Mol Biol*. 2018;1790:165–180. doi:10.1007/978-1-4939-7860-1_13
32. Keu KV, Witney TH, Yaghoubi S, et al. Reporter gene imaging of targeted T cell immunotherapy in recurrent glioma. *Sci Transl Med*. 2017;9(373):eaag2196. doi:10.1126/scitranslmed.aag2196

33. Dubey P, Su H, Adonai N, et al. Quantitative imaging of the T cell antitumor response by positron-emission tomography. *Proc Natl Acad Sci U S A*. 2003;100(3):1232–1237. doi:10.1073/pnas.0337418100
34. Herschman HR. PET reporter genes for noninvasive imaging of gene therapy, cell tracking and transgenic analysis. *Crit Rev Oncol Hematol*. 2004;51(3):191–204. doi:10.1016/j.critrevonc.2004.04.006
35. Gschweng EH, McCracken MN, Kaufman ML, et al. HSV-sr39TK positron emission tomography and suicide gene elimination of human hematopoietic stem cells and their progeny in humanized mice. *Cancer Res*. 2014;74(18):5173–5183. doi:10.1158/0008-5472.can-14-0376
36. Yaghoubi SS, Jensen MC, Satyamurthy N, et al. Noninvasive detection of therapeutic cytolytic T cells with 18F-FHBG PET in a patient with glioma. *Nat Clin Pract Oncol*. 2009;6(1):53–58. doi:10.1038/ncponc1278
37. Traversari C, Marktel S, Magnani Z, et al. The potential immunogenicity of the TK suicide gene does not prevent full clinical benefit associated with the use of TK-transduced donor lymphocytes in HSCT for hematologic malignancies. *Blood*. 2007;109(11):4708–4715. doi:10.1182/blood-2006-04-015230
38. Moroz MA, Zhang H, Lee J, et al. Comparative analysis of T cell imaging with human nuclear reporter genes. *J Nucl Med*. 2015;56(7):1055–1060. doi:10.2967/jnumed.115.159855
39. Zhang H, Huang R, Pillarsetty N, et al. Synthesis and evaluation of 18F-labeled benzylguanidine analogs for targeting the human norepinephrine transporter. *Eur J Nucl Med Mol Imaging*. 2014;41(2):322–332. doi:10.1007/s00259-013-2558-9
40. Heidari P, Kunawudhi A, Martinez-Quintanilla J, Szretter A, Shah K, Mahmood U. Somatostatin receptor type 2 as a radiotheranostic PET reporter gene for oncologic interventions. *Theranostics*. 2018;8(12):3380–3391. doi:10.7150/thno.24017
41. McCracken MN, Vatakis DN, Dixit D, McLaughlin J, Zack JA, Witte ON. Noninvasive detection of tumor-infiltrating T cells by PET reporter imaging. *J Clin Invest*. 2015;125(5):1815–1826. doi:10.1172/jci77326
42. McCracken MN, Gschweng EH, Nair-Gill E, et al. Long-term in vivo monitoring of mouse and human hematopoietic stem cell engraftment with a human positron emission tomography reporter gene. *Proc Natl Acad Sci U S A*. 2013;110(5):1857–1862. doi:10.1073/pnas.1221840110
43. Ponomarev V, Doubrovin M, Lyddane C, et al. Imaging TCR-dependent NFAT-mediated T-cell activation with positron emission tomography in vivo. *Neoplasia*. 2001;3(6):480–488. doi:10.1038/sj.neo.7900204
44. Strand J, Honarvar H, Perols A, et al. Influence of macrocyclic chelators on the targeting properties of (68)Ga-labeled synthetic affibody molecules: comparison with (111)In-labeled counterparts. *PLoS One*. 2013;8(8):e70028. doi:10.1371/journal.pone.0070028
45. Hosse RJ, Rothe A, Power BE. A new generation of protein display scaffolds for molecular recognition. *Protein Sci*. 2006;15(1):14–27. doi:10.1110/ps.051817606
46. Radu CG, Shu CJ, Nair-Gill E, et al. Molecular imaging of lymphoid organs and immune activation by positron emission tomography with a new [18F]-labeled 2′-deoxycytidine analog. *Nat Med*. 2008;14(7):783–788. doi:10.1038/nm1724
47. Higashikawa K, Yagi K, Watanabe K, et al. ^{64}Cu-DOTA-anti-CTLA-4 mAb enabled PET visualization of CTLA-4 on the T-cell infiltrating tumor tissues. *PLoS One*. 2014;9(11):e109866. doi:10.1371/journal.pone.0109866
48. Vento J, Mulgaonkar A, Woolford L, et al. PD-L1 detection using 89Zr-atezolizumab immuno-PET in renal cell carcinoma tumorgrafts from a patient with favorable nivolumab response. *J Immunother Cancer*. 2019;7(1):144. doi:10.1186/s40425-019-0607-z